Chapter 4

Imaging with multiples using LSRTM

In this chapter, I present a technique for imaging both primaries and higher-order multiples using joint least-squares reverse-time migration (joint-LSRTM). As discussed in chapter 1, one critical challenge with multiple imaging is the presence of crosstalk artifacts in the migration image. By enforcing the consistency between synthetics and observed data, joint-LSRTM can better delineate between true reflectors and noise in the image. When used with a suitable migration velocity model, this technique uses the multiple energy as signal. I can image a class of multiply scattered events by using the two-way propagator in both modeling and migration. Such events can scatter off sharp-interfaces in the migration velocity as well as the sea surface.

I will begin by discussing the theory for the ocean bottom node (OBN) acquisition geometry. An illumination analysis of the primary and multiples will be presented. I will show the effect of joint-LSRTM as compared to migration on a simple 2D layered model. Finally, I will demonstrate the concept and methodology in 2D with a synthetic Sigsbee2B model. By including the multiples into imaging, I found that the image quality improved in areas close to the complex salt structures.

THEORY

Least-squares migration poses the imaging problem as an inversion problem by linearizing the wave-equation with respect to the image model ($\mathbf{m}$) In Appendix A, I show how to linearize the wave-equation to obtain the forward modeling and its adjoint operator. For simplicity, I will refer to the Born modeling operator as $\mathbf{L}$. The standard objective function measures the least-squares difference between the modeled data ($\mathbf{d}_{\text{mod}}$) and the observed data ($\mathbf{d}_{\text{obs}}$),

$$S(\mathbf{m}) = \|\mathbf{d}_{\text{mod}} - \mathbf{d}_{\text{obs}}\|^2 = \|\mathbf{Lm} + \mathbf{d}_o - \mathbf{d}_{\text{obs}}\|^2. \tag{4.1}$$

where the modeled data is the sum of the background data ($\mathbf{d}_o$) and the Born modeled data ($\mathbf{Lm}$). The background data is the full-wave modeling of the data based on the migration velocity. This background data term was discussed in detail in relation to salt-dimming in Chapter 3.

Multiple imaging with ocean-bottom node

In an ocean-bottom survey, the signal can be classified into up-going (Figure 4.1a) and down-going signal (Figure 4.1b-d) with respect to the receivers. The lowest order of the up-going signal is the primary reflection (Figure 4.1a). The lowest order of the down-going signal is the direct-arrival. Since the direct-arrival does not carry any information about the subsurface, the next order of down-going event, the mirror signal (Figure 4.1b), is used for conventional migration of down-going OBN data.

The focus of this chapter is on imaging the higher-order surface-related multiples (Figure 4.1c and d) for OBN data. In particular, I compare the image output between migration with the mirror data and joint-LSRTM with both mirror and multiple data. For the remaining of this chapter, I will refer to the first order down-going reflection (Figure 4.1b) as the mirror reflection and the surface-related down-going multiple reflections (Figure 4.1c and d) as the double-mirror reflections. Although

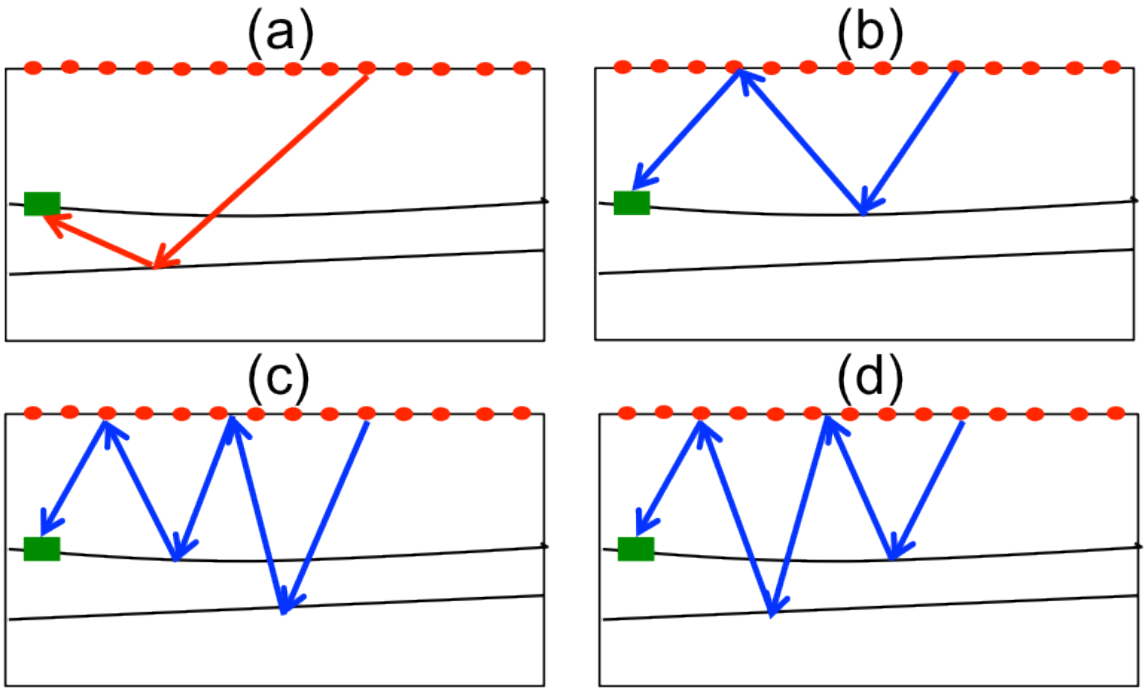

Figure 4.1: Ray-paths for (a) a primary reflection, (b) a mirror reflection, and (c, d) higher-order surface-related multiple reflections. [**NR**] chap4/. chap4-figure1

what I call the double-mirror reflections actually include all higher-order surface-related reflections, the strongest of such multiples involve two bounces off the sea-surface. Hence the word 'double' will be used to mark the most significant part of the higher-order multiple energy.

To jointly image with both mirror and double-mirror signals, I use the following objective function:

$$S(\mathbf{m}) = \|\mathbf{L}_{\text{mirror}}\mathbf{m} - \mathbf{d}_{\text{mirror}}\|^2 + \|\mathbf{L}_{\text{double}}\mathbf{m} - \mathbf{d}_{\text{double}}\|^2. \tag{4.2}$$

$\mathbf{L}_{\text{mirror}}$ and $\mathbf{L}_{\text{double}}$ are the linearized Born modeling operators for the mirror reflection and the double-mirror reflection events respectively. The recorded mirror and double-mirror data are represented by $\mathbf{d}_{\text{mirror}}$ and $\mathbf{d}_{\text{double}}$, respectively. Figure 4.2 describes the procedure for modeling mirror data. The procedure uses the symmetry across the sea surface to simulate one part of the traveling path. This concept was introduced in mirror imaging (Godfrey et al., 1998; Ronen et al., 2005). Figure 4.3 describes the procedure for modeling the double-mirror data. For the incident wavefield, the down-going data is used as an areal shot to simulate the first three legs of the travel path.

At first glance, $\mathbf{L}_{\text{mirror}}$ seems to only generate singly scattered events (e.g. Figure 4.4a). To clarify, the term scattering includes both diffraction and reflection. However, if I propagate the wavefields using the two-way wave equation, the Born modeling operator can actually generate multiply scattered events. In Figures 4.4b and d, the ray path reflects off a salt flank and then the horizontal reflector. If the sharp salt-flank boundary already exists in the migration velocity, then the scattering off the salt flank is automatically generated by the propagator. By using the data as a source, $\mathbf{L}_{\text{double}}$ can generate all higher-order surface-related multiples (Figure 4.4c).

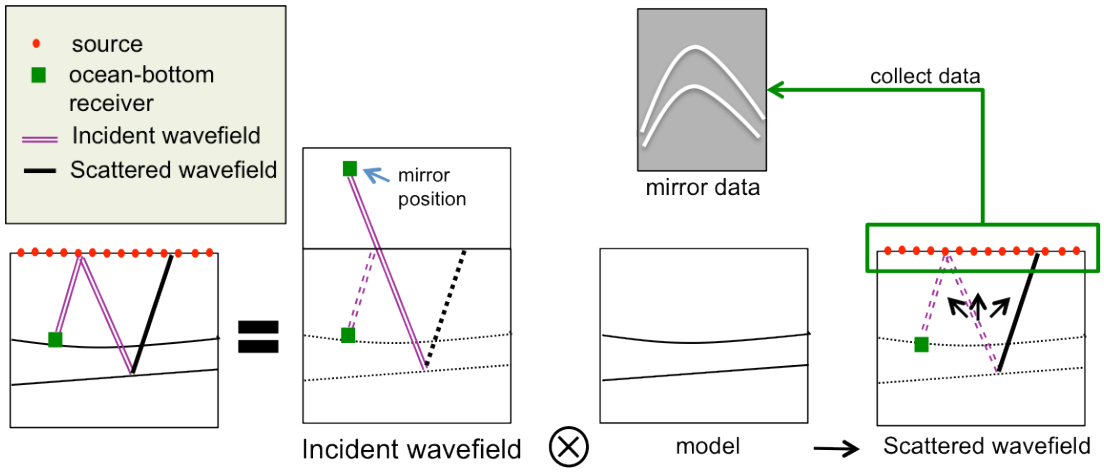

Figure 4.2: Born modeling of the mirror OBN data. The mirror reflection ray path can be divided into the incident part and the scattered part. To simulate the down-going leg of the ray path, OBN are placed at the mirror position with respect to the sea surface. The algorithm involves cross-correlating the incident wavefield with the image model to generate the input for the scattered wavefield. Synthetic mirror data is then collected at the sea surface (green box). [**NR**] chap4/. mirrorOp

ILLUMINATION ANALYSIS OF MULTIPLES

I performed an illumination analysis of the mirror and the multiples signal from the Sigsbee2B model. Figure 4.5 shows two sets of illumination angle gathers (Gherasim et al., 2014). The illumination angle gathers are calculated by placing scatterers near and under a complex salt body in the Sigsbee2B model. Each scatterer has a perfect amplitude-versus-angle (AVA) signature between 0 to 80 degrees. I apply Born modeling followed by reverse-time migration based on two types of reflection events. One type of event contains only the mirror reflection, and the other type contains only the double-mirror reflections. Figures 4.5a and b show the resulting illumination angle-gathers based on the mirror reflections and the double-mirror reflections, respectively. The calculated AVA signature is displayed to the right of each scattering point. Bright areas are angle ranges that are well illuminated. Label 1 highlights an area that is poorly illuminated by the double-mirror signal but is well illuminated by the mirror signal. On the other hand, label 2 highlights an area that is poorly

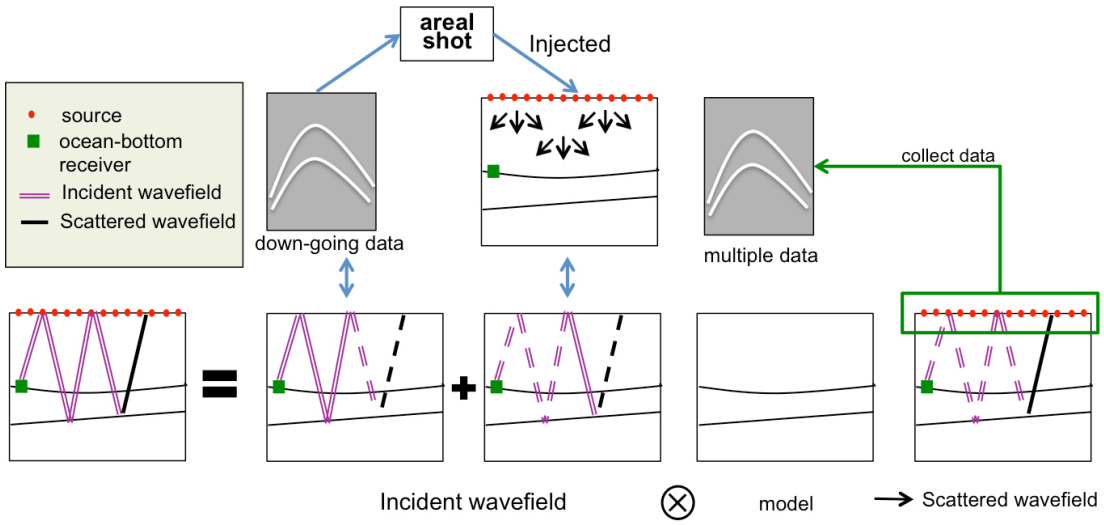

Figure 4.3: Born modeling of the higher-order surface-related multiples OBN data. For the incident wavefield, the down-going data is used as an areal shot to simulate the first three legs of the travel path. To generate the incident wavefield, the areal shot is injected at the sea-surface with a -1 factor. The procedure to generate the scattered wavefield is similar to that for the mirror reflection (Figure 4.2). [**NR**] chap4/. multipleOp

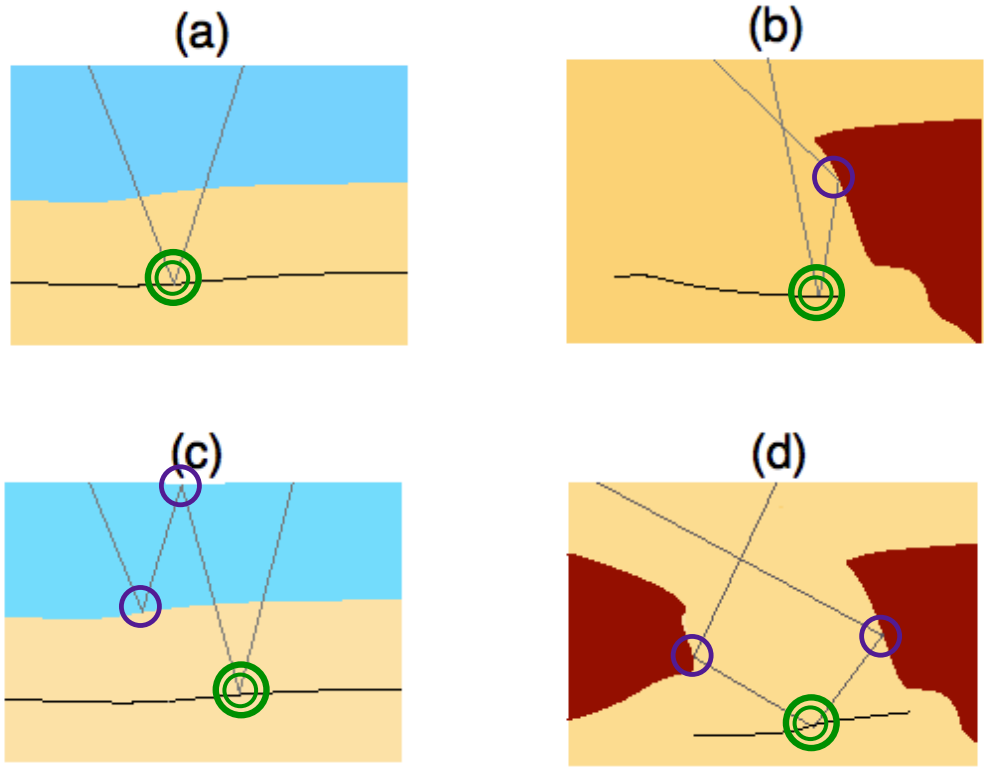

Figure 4.4: The ray-path for (a) a singly scattered event, (b) a doubly scattered event and (c,d) triply scattered events. Single circles (in purple) indicate scattering off the migration velocity and the sea surface. Double circle (in green) indicate scattering off the image model. [**NR**] chap4/. chap4-figure4

illuminated by the mirror signal but is well illuminated by the double-mirror signal. Label 3 points to areas that are illuminated by both the mirror and the double-mirror but at a different angular range.

We can better understand the illumination difference between the mirror and the double-mirror signal by examining the incident wavefield. Figure 4.6 shows a snapshot of the incident wavefield from the mirror and the double-mirror signals. Due to the rugosity of the salt, energy that enters the salt is often bent at different angles. In the mirror wavefield (Figure 4.6a) , we can see that the energy that enters the annotated shadow zone is weaker than energy in other parts of the model. On the other hand, the bending from the complex salt structure causes the energy from the double-mirror wavefield (Figure 4.6b) to enter the shadow zone at a different angle. This results in different angular illumination between the two types of signal as observed in Figure 4.5.

In general, the double-mirror illumination response (Figure 4.5) has a lower resolution than the mirror-illumination response. This is because of the cross-correlation imaging condition in RTM. Essentially, the double-mirror illumination response is composed of correlating multiple source wavelets and subsurface reflectivities. This problem will be addressed when using least-squares migration.

SYNTHETIC EXAMPLE

I apply joint-LSRTM on two models. The first one is a simple one-layered model that allows us to keep track of different kinds of migration artifacts. The second model is the more complicated Sigsbee2B model.

One-layered model

I construct a one-layered model (Figure 4.7 a) with ocean-bottom geometry. Figure 4.7 b shows the synthetic data. Label d_1 points to a mirror reflection, while labels d_2 and d_3 indicate higher order multiple events. Because I use Born modeling to generate

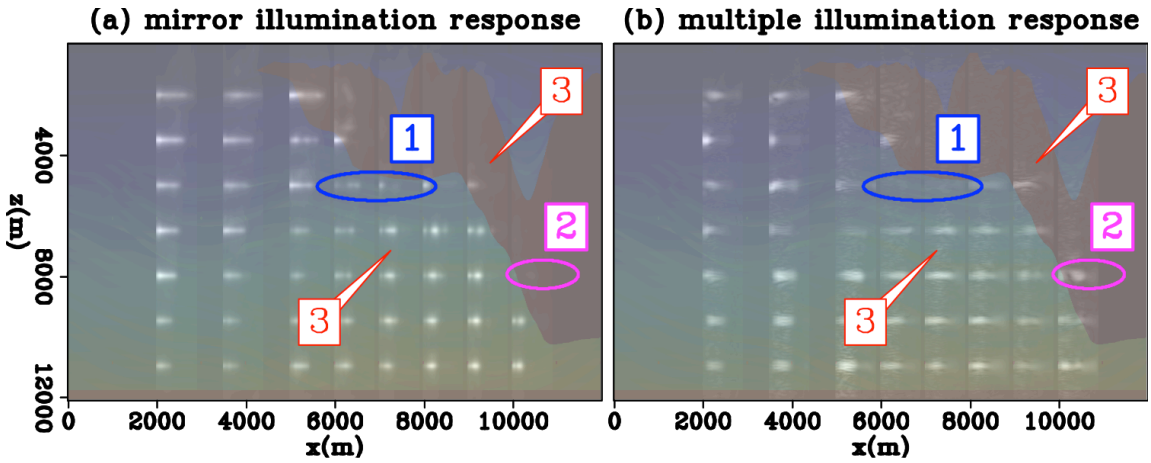

Figure 4.5: Illumination angle gathers based on (a) the mirror and (b) the multiple reflections. A set of scatterers are placed throughout the Sigsbee2B model. Each scatterer has a AVA signature from 0 to 80 degrees displayed to the right of the scattering point. Label 1 and 2 show areas that are poorly illuminated by the double-mirror and the mirror signals, respectively. Label 3 points to areas that are illuminated by both type of signals but at different angular range. [**NR**] chap4/. chap4-angillum

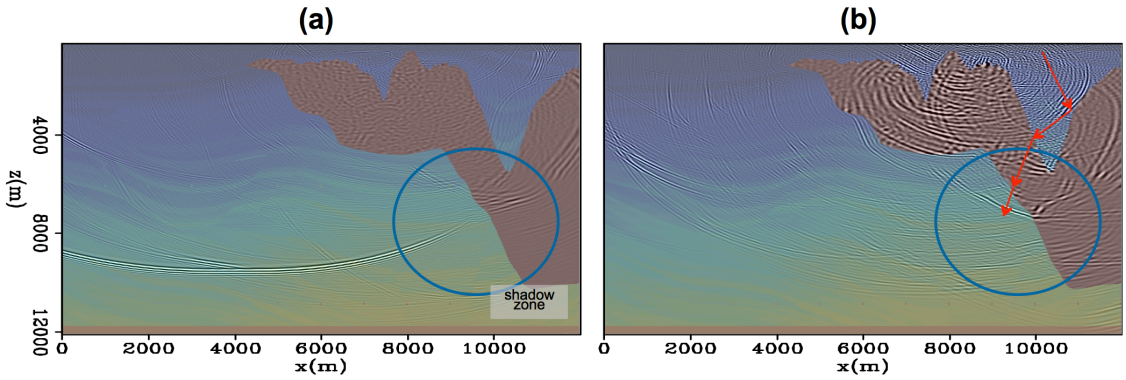

Figure 4.6: A snapshot of the incident wavefield from (a) the mirror and (b) the double-mirror signal.The two sets of wavefield enter the shadow zone with different angles and strength. [**NR**] chap4/. chap4-sigwfld2

the synthetic data, internal multiples are absent. Figure 4.7 c shows the migration image m_{mig}. The migration image is made up of signal m_{sig} and crosstalk artifacts m_{xtalk}. In the figure, label A marks spurious reflectors generated by migrating the mirror signal (d_1) as if it were a multiple. Label B highlights the correct reflector in the image. Label C points to an artifact generated by migrating the multiple signal (d_2 or d_3) as if it were a mirror reflection. In equation form, they are denoted as follows:

$$\begin{aligned} m_{mig} &= m_{signal} + [m_{xtalk}] = m_B + [m_A + m_C]\,, \qquad (4.3)\\ m_A &= \mathbf{L'}_2\mathbf{d}_1 + \mathbf{L'}_3\mathbf{d}_1 + \mathbf{L'}_4\mathbf{d}_1 + ...,\\ m_B &= \mathbf{L'}_1\mathbf{d}_1 + \mathbf{L'}_2\mathbf{d}_2 + \mathbf{L'}_3\mathbf{d}_3 + ...,\\ m_C &= \mathbf{L'}_1\mathbf{d}_2 + \mathbf{L'}_1\mathbf{d}_3 + \mathbf{L'}_2\mathbf{d}_3 + ..., \end{aligned}$$

where m_A, m_B,and m_C correspond to the parts of the image labeled with A, B, and C in Figure 4.7 c. $\mathbf{L'}_1$, $\mathbf{L'}_2$, and $\mathbf{L'}_3$ are migration operators that correspond to different orders of reflection events. Figure 4.7 d shows the inversion result. Notice that the artifacts are removed from the image. In conventional RTM, if there is residual multiple energy in the data, artifacts of type C would appear in the image. Treating it as real signal would negatively affect the interpretation of the sub-surface. Figure 4.7d shows the joint-LSRTM result. Joint-LSRTM poses the imaging problem as an inversion problem. Therefore, it enforces the consistency between observed and modeled data. Since the Born modeling operator has incorporated the kinematics of the multiples, the multiple energy in the data (d2 and d3) can now be properly explained. As a result the crosstalk artifacts in the RTM image is removed. Beside removing artifacts in the image, joint-LSRTM can improve the imaging in some poorly illuminated areas . In the next section, I will test the method on the 2D Sigsbee2B synthetic model where there are shadow zones underneath a complex salt overburden.

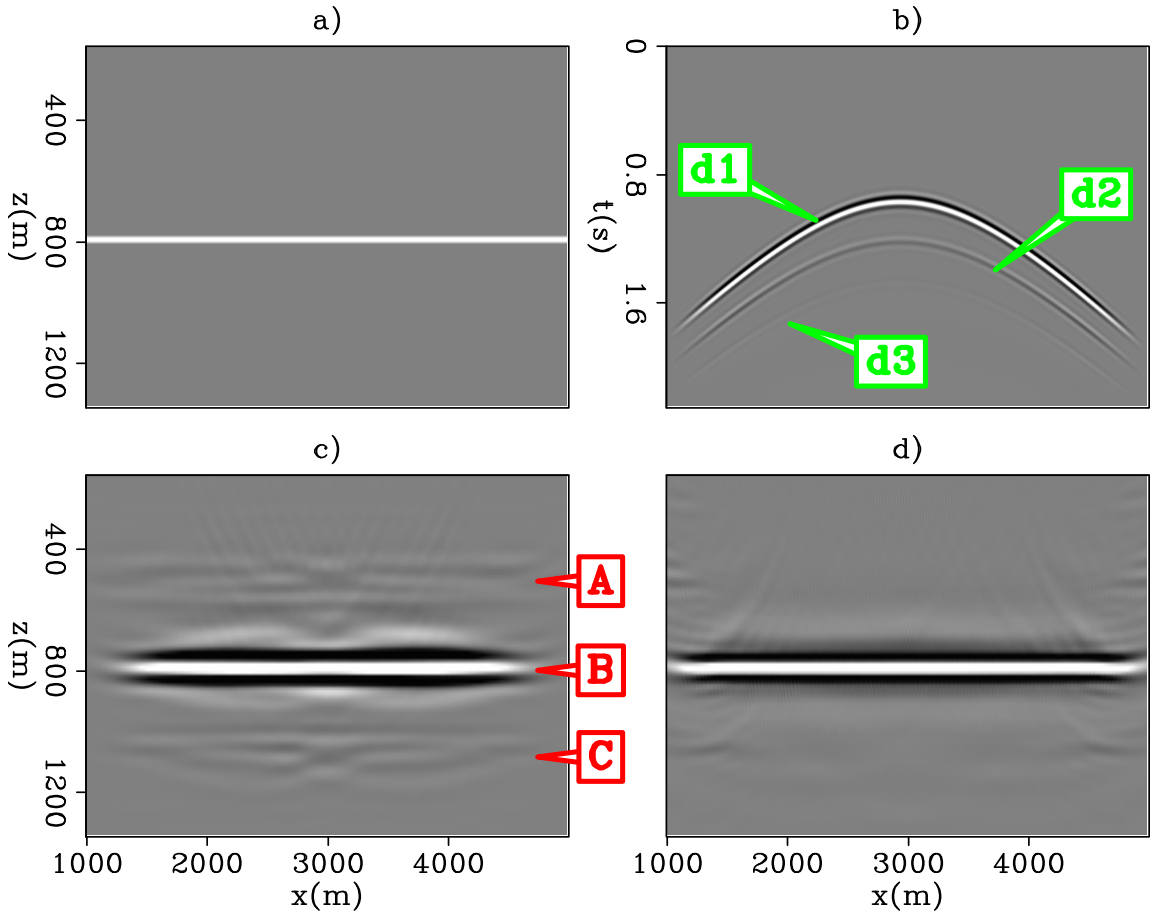

Figure 4.7: (a) Original one layered model, (b) synthetic data, (c) migration image and (d) inversion image. [**CR**] chap4/. Onelayerv2

Sigsbee2B model

I apply joint-LSRTM to the Sigsbee2B model with the ocean-bottom geometry. Figure 4.8 shows the migration velocity and the reflectivity model used for this study. There are two interfaces in the migration velocity. One comes from the salt and the other comes from the basement reflector. These sharp interfaces along with the free surface boundary condition will generate strong multiples in the data. I first generate the mirror data ($\mathbf{d}_{mirror} = \mathbf{L}_{\text{mirror}}\mathbf{m}$) using the procedure in Figure 4.2. It requires

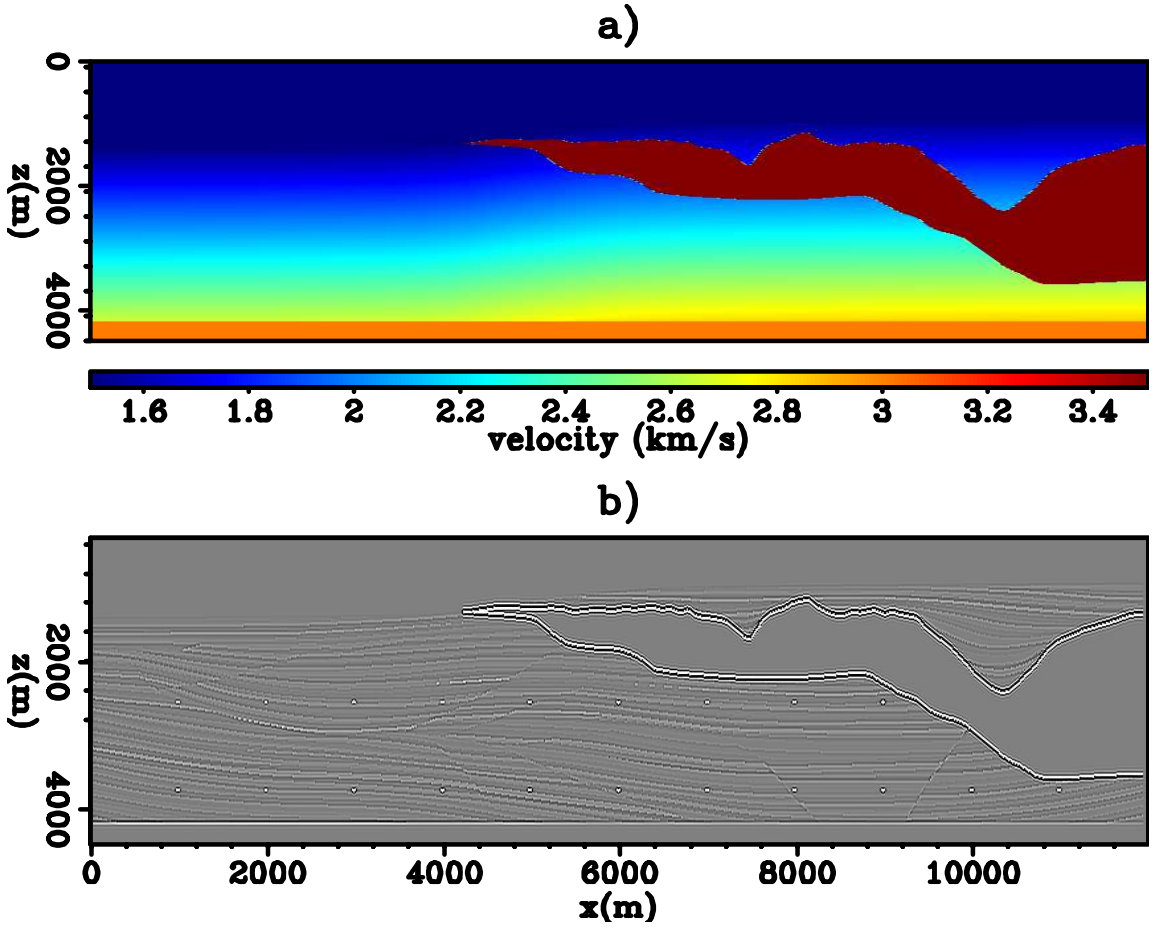

Figure 4.8: (a) Migration velocity model and (b) original reflectivity model. [**ER**] chap4/. panel1-m

positioning the nodes at the mirror point across the sea surface. In standard processing flow, surface-related multiples are often predicted and subtracted. Next, I use the synthetic double-mirror data ($\mathbf{d}_{double} = \mathbf{L}_{\text{double}}\mathbf{m}$) to represent the predicted multiples from the standard processing flow. I then add 20% of the double-mirror data to the mirror data. This is to simulate the case when multiple-elimination techniques cannot completely remove the multiples. I will refer to this synthetic simply as the noisy-mirror data (Figure 4.9a). Figure 4.9 (b) shows the synthetic that are the sum of mirror and double-mirror data.

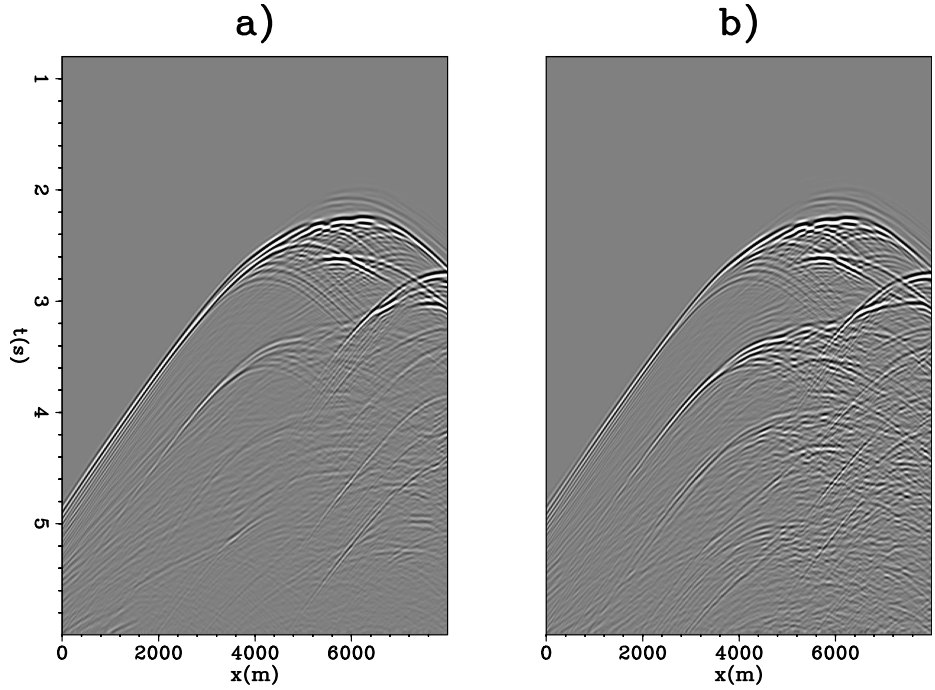

Figure 4.9: (a) The synthetic mirror data with 20 % double-mirror energy (*the noisy-mirror data*). (b) The synthetic data with both mirror and double-mirror reflections. [**CR**] chap4/. chap4-dataCom

Next, I perform three different types of inversion. The first inversion, termed as the Mirror-LSRTM, tries to match the noisy-mirror data using mirror-modeling operator. The double-LSRTM tries to match the double-mirror data with the double-mirror modeling operator. Finally, the joint-LSRTM uses both the mirror and the double-mirror signal as described in equation 4.2 to produce a single image.

Figure 4.10 shows the result of applying RTM and LSRTM. Figure 4.10a is the mirror-RTM image. Label 1 indicates the artifacts in the migration image that correspond to crosstalk noise. The artifacts overshadow a bright spot in the image. Figure 4.10b is the mirror-LSRTM result. Note the substantial improvement in the crosstalk noise between migration and inversion. Although LSRTM can enhance the resolution of the image ((Wong et al., 2011)), poorly illuminated areas still struggle. The subsalt area is not well illuminated (Box 2). Next, Figure 4.10c shows the result obtained

by applying LSRTM to the double-mirror signal. Even with inversion, the sediment area remains poorly illuminated (Box 3). Finally, Figure 4.10d is calculated using joint-LSRTM (equation 4.2). The image is superior to other imaging result in all 3 highlighted regions.

Figure 4.11 shows a deeper area of the Sigsbee2B model. Label 1 indicates an area underneath the complex salt structure, while label 2 highlights an area against a salt flank. Both areas are better imaged with joint-LSRTM of mirror and double-mirror signals than by other techniques (Figure 4.11a-d).

In terms of convergence, our objective function decreases to two percent of its initial value after 40 iterations. The inversion converges pretty quickly because the modeling operator used in the inversion is exactly the same as the modeling operator used to generate the observed data. For field dataset application , additional weighting and regularization to the inversion problem are needed for faster convergence.

DISCUSSION

Joint LSRTM does not migrate all orders of multiples. It only migrates multiples associated with surface-related reflection or scattering off sharp velocity interfaces such as the sediment-salt transition. Considering that multiples with high-amplitude in the data are often generated by subsurface interfaces of high impedance contrast, this technique can account for most of the significant multiples in the data.

This method is model-based. One consideration is the accuracy of the migration velocity. Because the operators in LSRTM are based on the linearization of the wave-equation, strong deviation between the migration velocity and the true velocity would hamper the effectiveness of this technique. However, using the double-mirror in LSRTM as described is no more sensitive to the velocity than primary-LSRTM or mirror-LSRTM. This is because field datasets are used as an areal source in the multiple modeling operator. Both the waveform and the travel time is correct up to the last down-going and up-going legs of a multiple reflection. If the migration velocity is good enough for mirror-LSRTM to improve over RTM, then double-LSRTM

or joint-LSRTM should also produce improved images.

CONCLUSION

I demonstrated a method for imaging with surface-related multiples using joint-LSRTM for ocean bottom node datasets. This technique increases the subsurface illumination by using the multiple energy as signal and it also addresses the issue of crosstalk in the image. I demonstrate the concept and methodology with a 2D layered model and the Sigsbee2B model.

ACKNOWLEDGMENTS

I thank Dave Nichols and Robert Clapp for suggestions and comments.

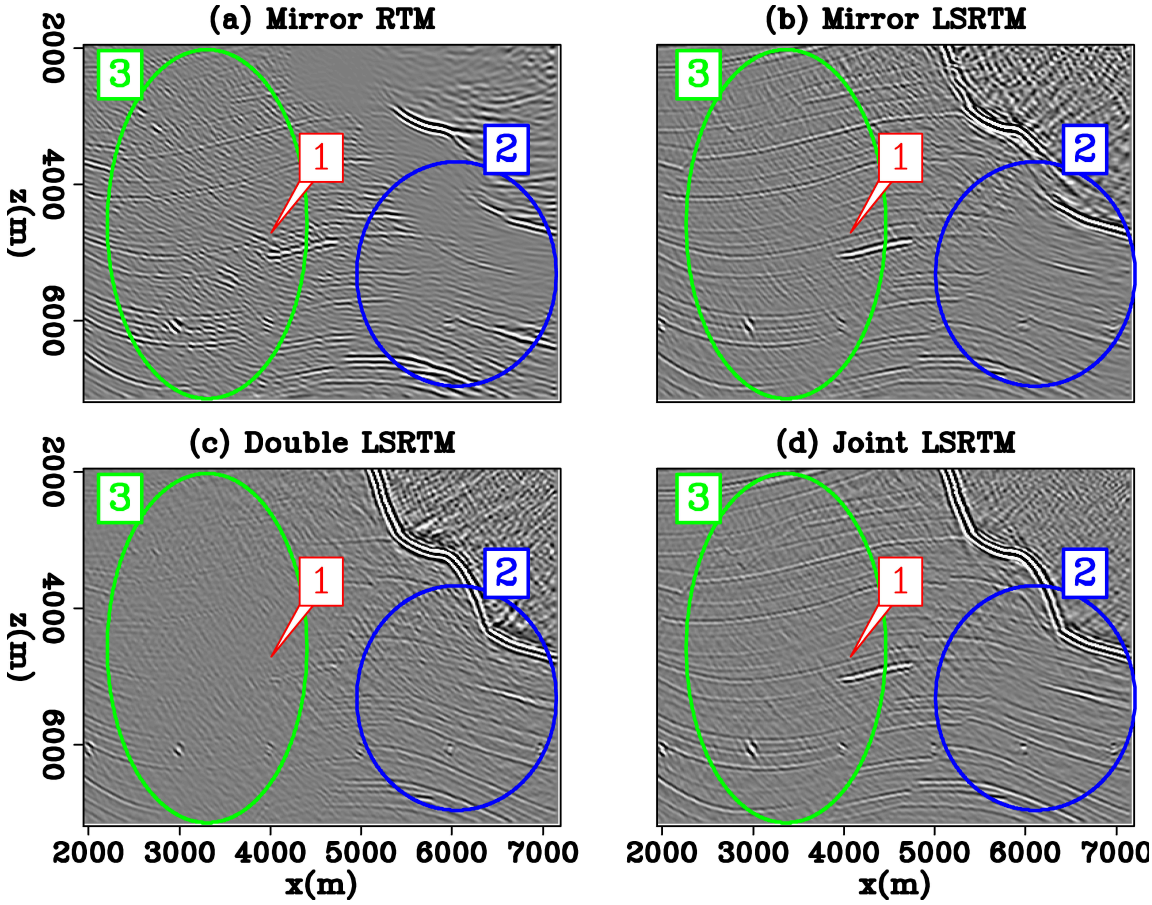

Figure 4.10: A section of the Sigsbee2B model from z=1950-7185 m and x=1950-7185 m calculated using (a) Mirror-RTM, (b) Mirror-LSRTM, (c) Double-mirror LSRTM, and (d) joint-LSRTM. Label 1 indicates a strong crosstalk noise in the Mirror-RTM. Label 2 highlights a subsalt area that is poorly illuminated by the mirror signal but is well illuminated by the double-mirror signal. Label 3 marks a sediment area that is poorly illuminated by the double-mirror signal but is well illuminated by the mirror signal. [**CR**] chap4/. chap4-sigsbee1

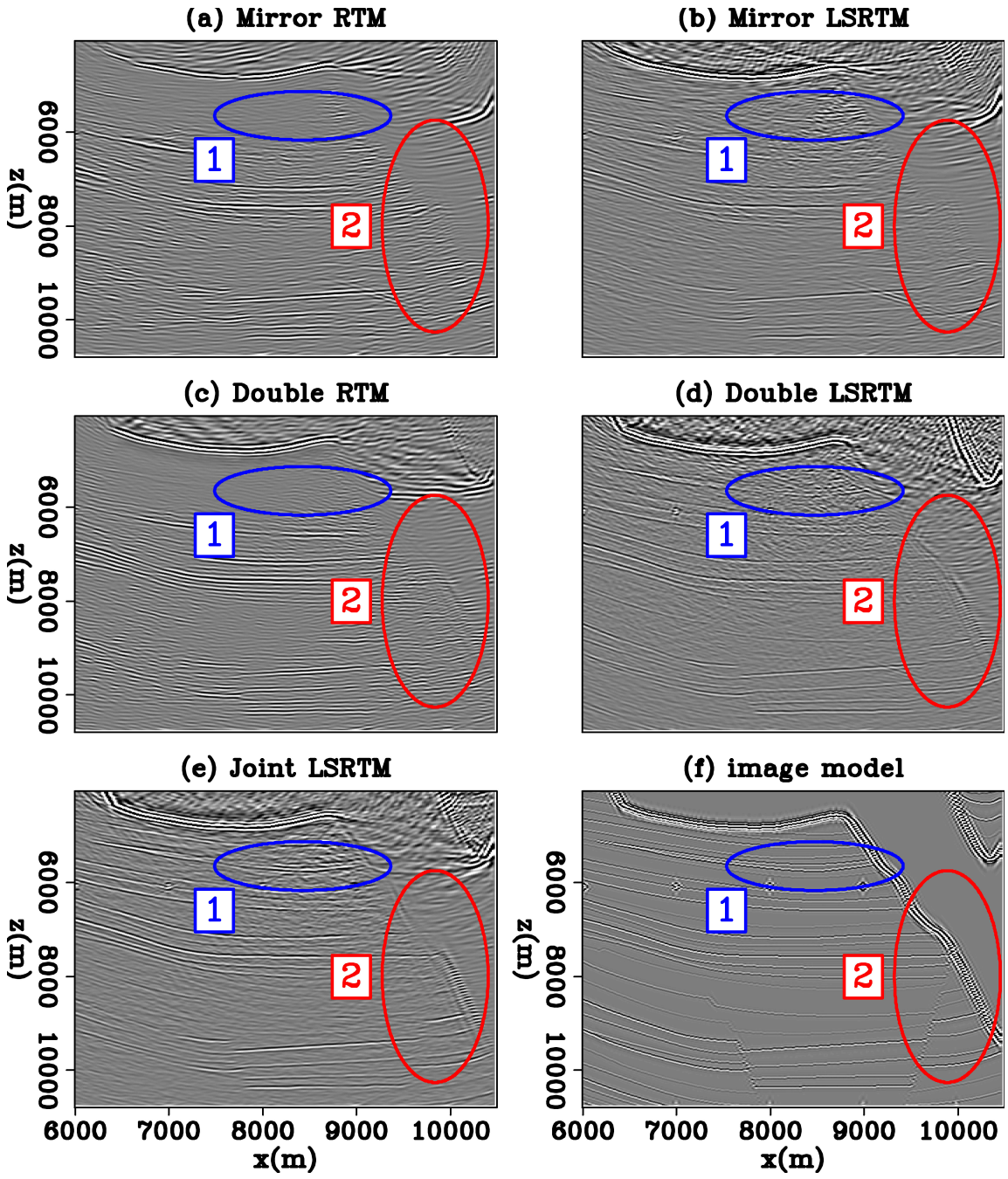

Figure 4.11: A section of the Sigsbee2B model from x=6000-10485 m and z=4050-10785 m calculated using (a) mirror-RTM, (b) mirror-LSRTM, (c) double-mirror-RTM, (d) double-mirror-LSRTM, and (e) joint-LSRTM. (f) is the original image. Labels 1 and 2 highlight two areas against the salt that are better imaged with joint-LSRTM. [**CR**] chap4/. chap4-sigsbee2